On the Influence of Electrolyte Cations on Electron Transport and Electron Transfer in Dye-Sensitized Solar Cells

Hongxia Wang*,[1] and Laurence M. Peter

Department of Chemistry, University of Bath, Bath, BA2 7AY, United Kingdom

AUTHOR EMAIL ADDRESS: hx.wang@qut.edu.au

RECEIVED DATE

[1] Current address: School of Chemistry, Physics and Mechanical Engineering, Queensland University of Technology, Brisbane QLD 4001, Australia

ABSTRACT

The influence of different electrolyte cations ((Li^+, Na^+, Mg^{2+}, tetrabutyl ammonium (TBA^+)) on the TiO_2 conduction band energy, E_c, the effective electron lifetime (τ_n) and the effective electron diffusion coefficient (D_n) in dye-sensitized solar cells (DSCs) was studied quantitatively. The separation between E_c and the redox Fermi level, $E_{F,redox}$, was found to decrease as the charge/radius ratio of the cations increased. E_c in the Mg^{2+} electrolyte was found to be 170 meV lower than in the Na^+ electrolyte and 400 meV lower than in the TBA^+ electrolyte. Comparison of D_n and τ_n in the different electrolytes was carried out by using the trapped electron concentration as a measure of the energy difference between E_c and the quasi Fermi level, ${}_nE_F$, under different illumination levels. Plots of D_n as a function of the trapped electron density, n_t, were found to be relatively insensitive to the electrolyte cation, indicating that the density and energetic distribution of electron traps in TiO_2 are similar in all of the electrolytes studied. By contrast, plots of τ_n vs. n_t for the different cations showed that the rate of electron back reaction is more than an order of magnitude faster in the TBA^+ electrolyte compared with the Na^+ and Li^+ electrolytes. The electron diffusion lengths in the different electrolytes followed the sequence of $Na^+ > Li^+ > Mg^{2+} > TBA^+$. The trends observed in the AM 1.5 current-voltage characteristics of the DSCs are rationalized on the basis of the conduction band shifts and changes in electron lifetime.

KEYWORDS: dye-sensitized, electron lifetime, electron diffusion length, electrolyte cations.

Introduction

As a consequence of their potentially low production cost and improving energy conversion efficiency, dye-sensitized solar cells (DSCs) are considered promising candidates for the next generation of photovoltaic devices. A typical DSC consists of a mesoporous dye-coated TiO_2 electrode, an electrolyte containing I^-/I_3^- as redox couple, and a platinized counter electrode.[1] Under illumination, electrons are injected from dye molecules into the TiO_2 conduction band and are extracted by diffusion through the TiO_2 film to the current collector. Following electron injection, the dye is regenerated from its oxidized state by electron transfer from I^- in the electrolyte, and I_3^- ions formed in the regeneration process diffuse to the counter electrode, where they accept electrons to complete the regenerative cycle.

The influence of cations on DSC characteristics has been discussed widely in the literature. In their landmark Nature paper in 1991, O'Regan and Grätzel reported that the incident photon-to-current conversion efficiency (IPCE) of the DSC increased from 68% to 84% when using Li^+ to replace tetrapropylammonium in the electrolyte.[2] The effect of alkali metal cations on the performance of DSCs was investigated later by Liu *et al.*[3], who observed that the photocurrent decreased while the photovoltage increased with increasing ionic radius of the cations. This phenomenon was attributed to changes of the TiO_2 conduction band energy, E_c, and the associated influence on electron injection efficiency, although the authors provided no specific experimental evidence for this hypothesis. The shift of E_c brought about by 'potential determining' cations such as Li^+, Na^+ and Mg^{2+} was later reported by Redmond *et al.*, who measured the flatband potential, V_{fb}, of TiO_2 films in acetonitrile solutions containing 0.1 M different cations using a three-electrode system. They found that V_{fb} in the Mg^{2+} electrolyte was 20 mV lower than in Li^+ electrolyte and 95 mV lower than in the Na^+ electrolyte.[4] In aqueous solution, the V_{fb} of TiO_2 is determined by the proton concentration, following the Nernstian relationship V_{fb} = -0.4 – (0.059× pH) V vs. SCE. [5] Changes in electron injection efficiency associated with the presence of different cations in the electrolyte were investigated by Kelly *et al.* using a dye-coated TiO_2 film.[6] They found that the quantum yield for charge injection increased with the increasing

charge/radius ratio of the cations and explained this phenomenon in terms of improved energy overlap between the TiO_2 acceptor state (conduction band) and the dye LUMO level according to Marcus-Gerischer theory.[7] Pelet *et al*. reported that dye regeneration was accelerated by small cations like Mg^{2+}, Li^+ and Na^+ in the electrolyte,[8] and similarly Olson reported that the dye cation lifetime was reduced by small cations like Li^+ under bias potential and explained this by the charge density dependence of the rate of electron recombination with dye cation.[9] It is worth noting that all of the above observations were based on dye-coated TiO_2 films rather than complete DSCs, where the effects of cations are reported to be different.[10] Kambe *et al*. discussed cation effects on the diffusion coefficient of DSCs in terms of ambipolar diffusion and confirmed that the effective diffusion coefficient obtained for conventional concentrations of cations (above 0.1 M) was indeed due to electron transport.[11] In terms of DSC performance, Nakada *et al.* reported that the stability of the devices could be improved by appropriate selection of the cations in the electrolyte.[12] A systematic investigation into the influence of cations with variable charge density (charge to radius ratio) on the photovoltaic performance of DSCs was reported by Wang *et al*. [13] These authors found that the short circuit current was strongly dependent on the charge density of the cations.

An understanding the influence of electrolyte cations on the kinetics of electron transport and electron transfer of DSCs is important for both fundamental research and practical device optimization. However, comparative studies are complicated by the need to identify an appropriate set of standard conditions. Nakade *et al.* have reported a number of studies of the influence of different cations on the effective electron lifetime, τ_n, and effective electron diffusion coefficient, D_n.[11,12,14-16] These authors obtained τ_n and D_n by measuring small amplitude transients at open circuit and at short-circuit respectively, using the short-circuit photocurrent density, j_{sc} as a reference. Since it is known that the E_c of TiO_2 depends significantly on the electrolyte cation through adsorption/intercalation, it is important to find a basis for comparison that takes this into account. With improved understanding of the role of electron trapping in the DSC, it has become clear that τ_n and D_n values should be compared for the same

position of the quasi-Fermi level relative to the conduction band energy. A practical way of doing this is to make comparisons of τ_n and D_n as a function of the concentration of trapped electrons, provided that the trap distribution is the same in all the systems studied.[17] Since this approach has not been used systematically in previous work on the effects of cations of DSC performance, it is important to revisit this topic in order to obtain a self-consistent picture.

The cations in the DSC electrolyte can also affect other processes. A recent study by Li *et al.* found that the optical band gap of the organic dye C218 was strongly affected by the cations in the electrolyte as evidenced by the bathochromatic effect with Li^+ compared to dimethylimidazolium ion.[18] However, no such effect of cations was observed with the ruthenium complex dye C106.[19] The present investigation sets out to distinguish quantitatively between indirect effects due to shifts of E_c relative to the redox Fermi level, $E_{F,redox}$, and effects associated with the kinetics of transport and transfer of free conduction band electrons arising from cations in the case of DSCs employing the widely used N719 dye. The influence of cations including Li^+, Na^+, $Mg^{2+}$and tetra-butylammonium (TBA^+) on the kinetics of electron transport and electron transfer in the DSCs was investigated in detail. It was found that the E_c of the DSC with the presence of TBA^+ was ca. 400 meV higher than that of the DSC with Mg^{2+}. E_c in the presence of Na^+ is 80 meV higher than with Li^+. Investigation of electron transport showed that the cations appear to have a relatively small influence on D_n. By contrast, the rate of electron back reaction with I_3^- was found to depend strongly on the electrolyte cation. Surprisingly, the most rapid back reaction was observed for the DSC with the electrolyte containing TBA^+. Plots of τ_n vs. trapped electron density for electrolytes with Li^+ and Na^+ were over one order of magnitude higher than for TBA^+.

Theoretical

The study of transport and interfacial transfer of electrons in DSCs is complicated by the effects of

trapping/detrapping of electrons associated with a high density of trap states located in the band gap of TiO_2 film. The time constants for the relaxation of the free electron concentration following small amplitude perturbation under open circuit and short circuit conditions cannot be interpreted as the free electron lifetime $\tau_{n,0}$ and the free electron transit time $\tau_{t,0}$ respectively because the trapped electrons effectively 'buffer' the free electron concentration, leading to relaxation times that are much longer than $\tau_{n,0}$ and $\tau_{t,0}$. Bisquert and Vikhrenko have shown that the time constant, τ_n, for the relaxation of the free electron concentration is related to the free electron lifetime, $\tau_{n,0}$, by equation 1.[17]

$$\tau_n = \left(1+\frac{\partial n_t}{\partial n_c}\right)\tau_{n,0} = \left(1+\frac{\partial n_t}{\partial {}_nE_F}\frac{\partial {}_nE_F}{\partial n_c}\right)\tau_{n,0} = \left(\frac{k_BT}{N_c}\exp\left(\frac{E_c - {}_nE_F}{k_BT}\right)g\left({}_nE_F\right)\right)\tau_{n,0} \quad (1)$$

Here n_c is the concentration of free electrons, n_t is the concentration of trapped electrons, E_c is the conduction band energy, N_c is the density of conduction band states, ${}_nE_F$ is the quasi-Fermi level that determines the electron occupation of the trap and conduction band states and $g(E_T)$ describes the electron trap distribution. The trap distribution is often found to follow the exponential form[20]

$$g\left(E_T\right) = \frac{N_{t,0}}{k_BT}\exp-\left(\frac{E_c - E_T}{k_bT_0}\right) \quad (2)$$

where $N_{t,0}$ is the total density of trap states, E_T is the trap energy and k_BT_0 is an energy describing the width of the distribution. T_0 is commonly in the range 600-1200 K, so that τ_n decreases as ${}_nE_F$ moves towards the conduction band with increasing light intensity or externally applied voltage.

The trapping/detrapping model gives an apparent electron diffusion coefficient D_n that is related to $D_{n,0}$, the diffusion coefficient of free conduction band electrons, by the expression

$$D_n = \left(1+\frac{\partial n_t}{\partial n_c}\right)^{-1} D_{n,0} \quad (3)$$

Comparison of equations 1 and 3 shows that D_n increases as ${}_nE_F$ moves towards the conduction band with increasing light intensity or externally applied voltage. Provided that recombination is first order in the free electron density as assumed here, the electron diffusion length $L_n = (D_{n,0}\tau_{n,0})^{1/2}$ is identical with

$(D_n \tau_n)^{1/2}$ if D_n and τ_n are measured for the same value of $E_c - {}_nE_F$.

The dependence of both τ_n and D_n on $E_c - {}_nE_F$ poses a problem for comparative studies of the type described in the present paper. In practice, the energy difference E_c - ${}_nE_F$ is not readily accessible to measurement. Generally, the experimentally accessible quantity is the energy difference between the quasi-Fermi level and the redox Fermi level $E_{F,redox}$ (${}_nE_F$ - $E_{F,redox}$), which at open circuit corresponds to the photovoltage qU_{photo} (or open circuit voltage qV_{oc}). E_c - ${}_nE_F$ is related to qU_{photo} by

$$E_c - {}_nE_F = \left(E_c - E_{F,redox}\right) - qU_{photo} \tag{4}$$

This means that both τ_n and D_n (measured at the same open circuit voltage) are sensitive to changes in E_c relative to $E_{F,redox}$ arising from changes in the interfacial dipole potential associated with adsorption of ionic or polar species. In order to separate this effect from real changes in $\tau_{n,o}$ and $D_{n,0}$, it is necessary to choose a suitable reference system. The method used in this study for comparing E_c values in DSCs fabricated with electrolytes containing different cations is based on measuring the total concentration of trapped electrons n_t, by near-infrared transmittance.[20,21] The concentration of trapped electrons varies with applied potential or with illumination intensity since the trap occupancy (as well as the occupancy of the conduction band) is determined by ${}_nE_F$. In practice, the concentration of conduction band electrons is several orders of magnitude lower than the concentration of trapped electrons, which is given by

$$n_t = \int_{E_{F,redox}}^{\infty} f_{FD}(E) g(E)\, dE \approx \int_{E_{F,redox}}^{{}_nE_F} g(E) dE \tag{5}$$

where the approximate form corresponds to the 'zero Kelvin approximation' of the Fermi Dirac function, $f_{FD.}$

Let us assume in the first instance that the total concentration of traps, $N_{t,0}$ and the characteristic temperature T_0 are the same for the different electrolytes. In this case, $E_c - {}_nE_F$ is constant for measurements made under conditions in which the trapped electron concentration is the same for the different electrolytes. Provided that $D_{n,0}$ is independent of the nature of the electrolyte,[22] this critical

assumption can be tested by comparing plots of D_n *vs.* n_t for different electrolyte cations. If the assumption is correct, all of the plots should coincide.

Experimental

Fabrication of dye-sensitized solar cells

Cleaned fluorine-doped tin oxide (FTO) conductive glass (TEC15, Libby Owens Ford, LOF) was coated with a thin compact layer of TiO_2 film by spray pyrolysis.[23] TiO_2 colloid films (Dyesol DSL-18-NR) were deposited onto the TiO_2 compact layer by doctor-blading, using 'Scotch' tape (3M) to control the thickness. The film was left in air to relax for 3-5 min before being sintered at 500^o C for 30 minutes. The sintered TiO_2 film was immersed in 40 mM aqueous $TiCl_4$ solution at 70^o C for 30 minutes, then resintered at 450^o C for 30 minutes after being thoroughly washed with Milli-Q water. The thickness of the TiO_2 film was ~13 μm as determined by a profilometer and the average area of the DSCs was 0.9 cm^2. Dye uploading was carried out by immersing the warm (about 80º C) TiO_2 film into the dye solution (0.25 mM *cis*-dithiocyanato bis(2,2$^{'}$-bipyridine-4,4$^{'}$-dicarboxylate) ruthenium-(II) *bis*-tetrabutylammonium (N-719, Dyesol) in acetonitrile/*tert*-butanol (1:1, V/V) for 16 hours. DSCs were assembled by sealing the dye-coated TiO_2 electrode and the thermally-platinized FTO (TEC 8, LOF) counter electrode together using a 25 μm thermoplastic gasket (Surlyn). Electrolyte was vacuum filled into the cells through holes in the counter electrode. The holes were then heat-sealed with microscope slips using Surlyn. The electrolytes with different cations (M^{n+} = Li^+, Na^+, Mg^{2+}, TBA^+) were composed of 0.5 M MI_n, 0.05 M I_2, 0.5 M *tert*-butylpyridine in acetonitrile/valeronitrile (85:15, V/V).

Characterization

The photovoltaic performance of the DSCs was measured under 1kW Xe solar simulator system (Müller) with an AM 1.5 filter. The incident power density was calibrated with a calibrated reference

silicon solar cell (Fraunhofer ISE) with a built-in KG5 filter to reduce spectral mismatch. Incident photon-to-current conversion efficiency (IPCE) spectra of the DSCs were measured in the spectral range of 400 – 800 nm with the resolution of 5 nm. A yellow filter was used to remove the second-order light diffraction at wavelengths longer than 550 nm.

Effective values of electron lifetimes and electron diffusion coefficients of the DSCs were measured by intensity modulated photovoltage spectroscopy (IMVS) at open circuit and intensity modulated photocurrent spectroscopy (IMPS) at short-circuit respectively under illumination.[24,25] A light-emitting diode (LED, 627 nm) was used to provide homogeneous monochromatic illumination across the TiO_2 cell, which was illuminated from TiO_2 electrode side. The ratio of the modulated illumination intensity to the DC illumination was 5% for both the IMVS and IMPS measurements.

The electron concentration in the DSCs was obtained by near-infrared transmittance in the dark by applying an external bias or under illumination with visible light (627 nm LED).[20,21,26] The voltage drop due to the current flowing across the cell was taken into account for measurements in the dark with external bias.

Results and discussion

DSC performance under AM 1.5 illumination

Figure 1 shows photocurrent density-voltage plots of DSCs fabricated with electrolytes containing different cations. The open circuit voltage, V_{oc}, of the DSCs follows the sequence of $TBA^+ > Na^+ > Li^+ > Mg^{2+}$, corresponding to increasing charge density of the cations (shown in the inset). The radii of Li^+, Na^+ and Mg^{2+} were taken from the WebElements Periodic Table, and the radius of the TBA^+ from literature [27]. This trend in V_{oc} is in good agreement with the observations by Liu *et al.*, who employed electrolytes composed of different alkali-iodides and iodine in a mixed ethylene carbonate/propylene carbonate solvent.[3] However, the short circuit photocurrent density, j_{sc}, of the DSCs measured in the present work does not vary in the reverse cation order reported by Liu *et al*.. In our case, the DSC with

Na^+ has the highest j_{sc} (j_{sc} = 9.9 mA cm^{-2}), whereas the TBA^+-based DSC has the lowest value (j_{sc} = 5.39 mA cm^{-2}). As a consequence, the cell fabricated with the Na^+-containing electrolyte shows the best power conversion efficiency. The difference between the present results and those of Liu *et al*. is probably arises from the inclusion in our electrolytes of *tert*-butylpyridine (TBP), which is known to raise the conduction band energy. Zhang *et al* have reported that TBP may affect the adsorption/intercalation of cations such as TBA^+ on the surface of TiO_2 film.[28] TBP evidently affects the impact of cations on the performance of corresponding DSC because a similar trend of j_{sc} was observed for alkali cations when using the same electrolyte composition as Liu *et al*. [29]

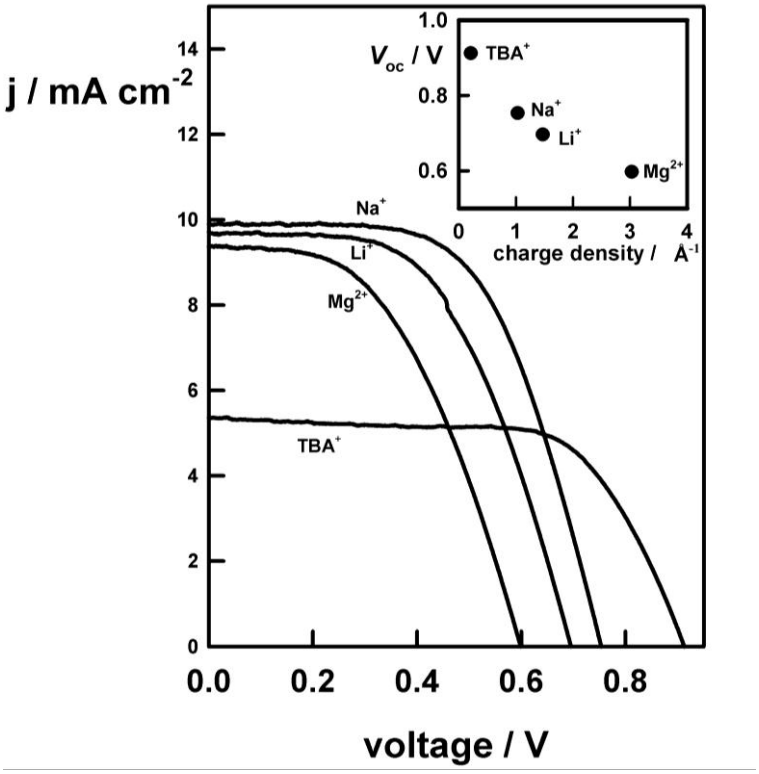

Figure 1. Current density-voltage plots of the dye-sensitized solar cells with different cations under AM 1.5 illumination (100 mW cm^{-2}). The inset shows how the open circuit voltage varies with the charge density of the cations in the electrolyte.

IPCE spectra

The IPCE spectra of DSCs based on electrolytes containing different cations are compared in Figure 2.

As can be seen, the peak IPCE values follow the sequence of $Na^+ > Li^+ > Mg^{2+} >> TBA^+$, which is consistent with the trends in j_{sc} in Figure 1. The differences in IPCE are less obvious at longer wavelengths, and this may be due to small differences in light scattering altering the effective optical path length. Strikingly, the TBA^+-based DSC shows a much lower IPCE over the whole spectrum.

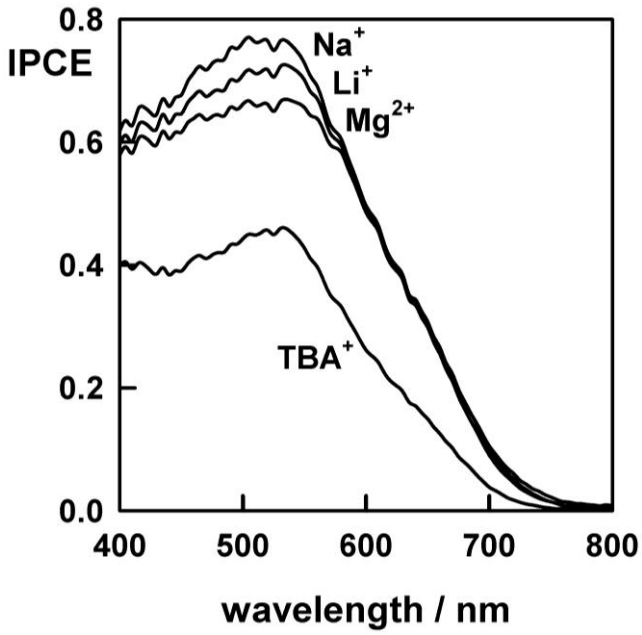

Figure 2. IPCE spectra of DSCs with electrolytes containing different cations.

The IPCE (corrected for optical losses) is the product of light harvesting efficiency (η_{lh}), the electron injection efficiency (η_{inj}) and the electron collection efficiency (η_{coll}).

$$IPCE = \eta_{lh}\eta_{inj}\eta_{coll} \tag{6}$$

η_{lh} is determined by the loading and extinction coefficient of the dye. The fact that the IPCE spectra of all the DSCs exhibit a similar onset indicates that that the optical band gap of the ruthenium complex N719 is not changed by the cations. η_{lh} should therefore be the same for all the cells because they have the same dye loading of the TiO_2 film. The observed differences in the peak IPCE must therefore reflect differences in η_{inj} and/or η_{coll}. η_{inj} is known to be sensitive to the energy overlap between the LUMO level of the dye molecule and the TiO_2 conduction band.[6,7,30] A lower TiO_2 conduction band relative to

the dye LUMO energy level is expected to enhance η_{inj} by increasing the driving force for the electron injection. η_{coll} is determined by the competition between the transport of electrons through the TiO_2 film and electron loss through back reaction with I_3^- and – if dye regeneration is slow – with oxidized dye molecules, D^+. The kinetics of electron transfer and transport in the TiO_2 film of the DSCs were therefore investigated in order to separate the influences of η_{inj} and η_{coll} on the IPCE and on j_{sc}.

Monitoring changes in conduction band energy

Figure 3 contrasts the concentrations of trapped electrons as a function of voltage (equivalent to ${}_nE_F - E_{F,redox}$) measured for the different electrolytes. With the exception of the plot for TBA^+, which is slightly steeper, the plots are parallel but are offset along the voltage axis with the sequence $Mg^{2+} < Li^+ < Na^+ < TBA^+$. The curvature, which is evidently the same for the series Mg^{2+}, Li^+, Na^+, indicates that the trap distribution is not exactly exponential (*cf.* equation 2). This is shown by the piecewise fits of the Na^+ data to equation 2 in the range 0.3 – 0.5 V and 0.5 – 0.8 V with different T_0 values (900 K and 1400 K respectively). The three orders of magnitude higher electron density for the Mg^{2+} based DSC than TBA^+ indicates that there is a strong accumulation of trapped electrons in cells with small electrolyte cations. The higher the charge density of the cations, the higher is the electron density in the corresponding DSC. This is in good agreement with the observation by Fredin *et al*.. [31]

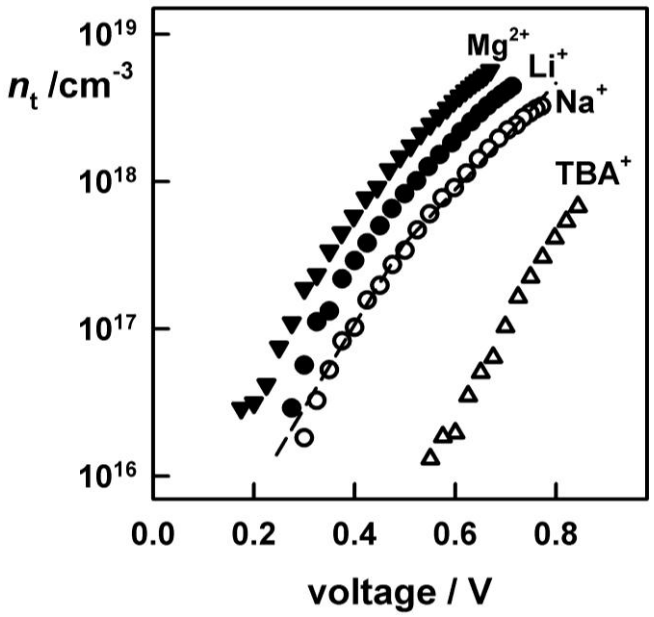

Figure 3. Voltage dependence of the trapped electron concentration in DSCs with different cations. The broken line shows the fits of the data for Na^+ to equation 2 over the ranges 0.3 - 0.5 V (T_0 = 900 K) and 0.5 - 0.8 V (T_0 = 1400 K).

If we assume for the present that the trap distribution (eq. 2) is unaffected by changes in cation, the voltage offsets seen in Figure 3 can be ascribed to shifts in $E_c - E_{F,redox}$. It follows that the differences in voltage *at constant* n_t correspond to the relative positions of E_c since $E_{F,redox}$ is constant in this work. Therefore, the TBA^+ electrolyte gives the highest E_c while Mg^{2+} gives the lowest. E_c in the presence of Mg^{2+} is 77 meV lower than with Li^+, and 178 meV and 400 meV lower than with Na^+ and TBA^+ respectively at $n_t = 3.0 \times 10^{18}$ cm^{-3}. The changes in E_c due to the different cations in the DSCs are much higher than the change of the V_{fb} reported for a dyed TiO_2 film in a three-electrode cell system.[4] Comparison of the shifts in E_c with the corresponding values of V_{oc} shown in Figure 1 shows that the trends are largely similar. For example, V_{oc} for the cell with Mg^{2+} is 90 mV lower than for Li^+ and 154 mV lower than for Na^+. This indicates that the change of the E_c induced by the cations is a major contributing factor responsible for the observed variation of V_{oc}. However, on closer inspection it can be seen that although E_c for TBA^+ is about 400 meV lower than for Mg^{2+}, the corresponding V_{oc} difference is only 310 mV. This indicates that the electron back reaction, τ_n, must also play a role in determining

the voltage performance of the cell.

Although injection efficiencies were not determined directly in the present work, we can make some predictions based on the trends in E_c. Since η_{inj} is sensitive to the energy difference between E_c of TiO_2 and the LUMO energy level of the dye molecule, the low E_c in the presence of Mg^{2+} is expected to lead to the highest η_{inj}. By the same reasoning, the DSC with the TBA^+ electrolyte should have the lowest η_{inj} because it has the highest E_c value. Based on the relative position of E_c, the η_{inj} values should follow the trend of $Mg^{2+} > Li^+ > Na^+ > TBA^+$.

The influence of E_c on V_{oc} can be explained as follows. The photovoltage measured under AM 1.5 illumination corresponds to the difference between the ${}_nE_F$ and $E_{F,redox}$. This difference depends on the free electron lifetime, $\tau_{n,0}$ and on the energy difference $E_c - E_{F,redox}$ according to Eq. 7 (where $U_{photo} = V_{oc}$).

$$\begin{aligned} qU_{photo} &= {}_nE_F - E_{F,redox} = \left(E_c - E_{F,redox}\right) + k_BT \ln \frac{n_c}{N_c} \\ &= \left(E_c - E_{F,redox}\right) - k_BT \ln N_c + k_BT \ln \frac{\eta_{inj} I_{abs}}{d} + k_BT \ln \tau_0 \end{aligned} \tag{7}$$

Here n_c is the concentration of conduction band electrons, N_c is the density of conduction band states and I_{abs} is the absorbed photon flux[1]. It follows from eq. 7 that a plot of V_{oc} *vs.* E_c - $E_{F,redox}$ for the different electrolytes should reveal differences in $\tau_{n,0}$ as deviations from linearity. Since $E_c - E_{F,redox} = ({}_nE_F - E_{F,redox}) + (E_c - {}_nE_F) = qU_{photo} + (E_c - {}_nE_F)$, we can plot V_{oc} vs. the voltage at which $E_c - {}_nE_F$ has a fixed value. This fixed value can be defined conveniently in terms of a fixed value of the trapped electron density, n_t. Figure 4 is a plot for the different electrolytes of V_{oc} *vs*. the voltage at which $n_t = 5 \times 10^{17}$ cm^{-3}. It can be seen that the points for the two alkali metal cations lie close to a line with unit slope, suggesting that the free electron lifetimes and electron injection efficiencies are similar for DSC with these two electrolytes. In other words, the differences in V_{oc} arise only from the shift in E_c. By contrast,

[1] Note that eq. 7 assumes that the DSC behaves ideally. The case of non-linear recombination is discussed in [32].

the V_{oc} values for Mg^{2+} and TBA^{+} fall well below the line, indicating that that η_{inj} and/or the free electron lifetime of the cell with Mg^{2+} and TBA^{+} are lower. This conclusion is confirmed by the lifetime measurements discussed below.

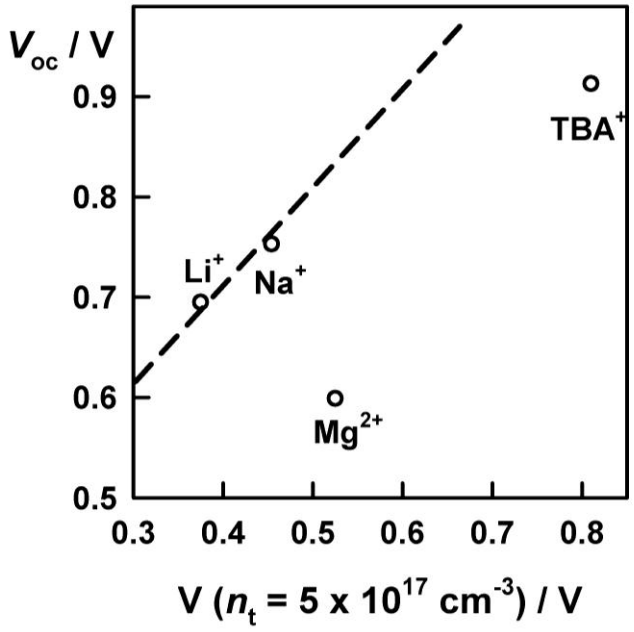

Figure 4. Open circuit voltage plotted *vs*. the voltage for which the trapped electron concentration $n_t = 5 \times 10^{17}$ cm^{-3}. The plot shows that the free electron lifetime is much lower in the Mg^{2+} and TBA^{+} electrolytes compared with Li^{+} and Na^{+}.

Comparison of trapped electron concentration under illumination at open circuit and short circuit.

Figure 5 compares the plots showing the concentration of trapped electrons for the Na^{+} electrolyte under open circuit and short circuit conditions. It can be seen that the plots are parallel, with the trapped electron concentration values at short circuit being an order of magnitude smaller than at open circuit. The difference indicates that ${}_nE_F$ is lower at short circuit than at open circuit. This has been confirmed in our previous work using a titanium sensor electrode and by near-IR transmittance [21,33-35] and also by Boschloo *et al.* by an interrupt technique.[36] The plot shown in Figure 5 can be used to estimate $\Delta_n E_F$, the

difference in mean ${}_nE_F$ values at open and short circuit, which corresponds to the horizontal translation on the voltage axis that is required to bring the two plots into coincidence. The Δ_nE_F values obtained for the different electrolytes were: Na^+ 190 meV; Li^+ 150 meV, Mg^{2+} 100 meV; TBA^+ 40 meV.

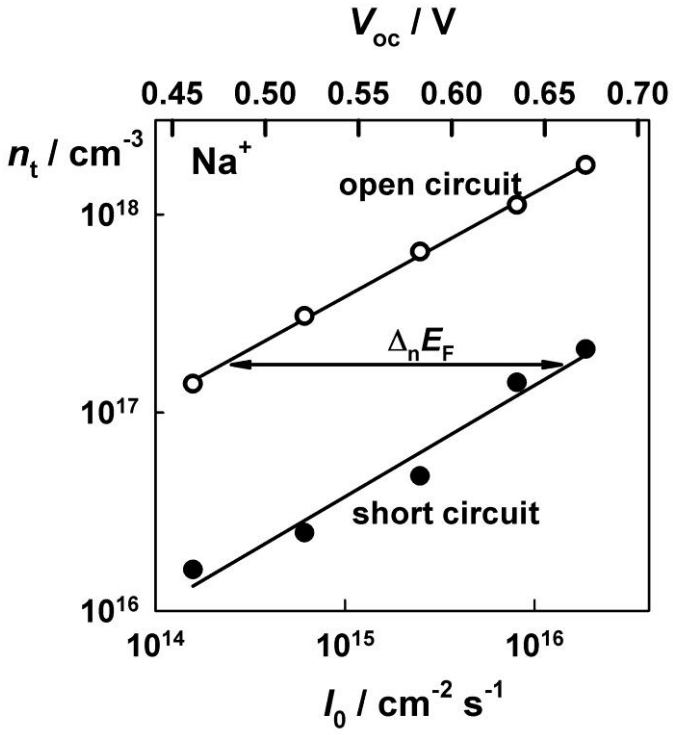

Figure 5. Comparison of the trapped electron concentration as a function of light intensity under short circuit and open circuit conditions for the DSC containing Na^+. The top scale is the corresponding open circuit photovoltage. The difference in quasi Fermi level is needed for the determination of the electron diffusion length by IMPS/IMVS.

Calculations of the free electron concentration profiles[33-35] based on solution of the continuity equation show that the difference in ${}_nE_F$ under open circuit and short circuit conditions is related to the electron diffusion length, $L_n = (D_{n,0}\tau_{n,0})^{1/2}$. A large value of Δ_nE_F corresponds to a long electron diffusion length. Since we expect $D_{n,0}$ to be the similar for all the electrolytes studied here, Δ_nE_F reflects primarily differences in $\tau_{n,0}$. Based on the measured Δ_nE_F values, the electron diffusion length decreases in the order $Na^+ > Li^+ >> Mg^{2+} > TBA^+$. As shown below, this is also the sequence observed in the plots of effective lifetime τ_n *vs*. n_t.

Comparison of D_n values

Plots of D_n *vs*. n_t for the DSCs with different cations are illustrated in Figure 6. If the trap distribution is indeed independent of the nature of the electrolyte cation, then these plots should all coincide, provided that $D_{n,0}$ is the same (we assume that the influence of the type of cations on the ambipolar diffusion coefficient is small since the concentration of electrons is many orders of magnitude lower than that of the cations.[37]). In fact the plots for all of the cations except Na^+ are reasonably coincident. The plot for Na^+ is slightly higher than for the other cations, suggesting that the assumptions of a cation-independent trap-distribution and constant $D_{n,0}$ may have limitations. The curvature seen in the plots reflects the fact that the trap distribution in these electrolytes is not exactly exponential, as can be seen in Figure 3.

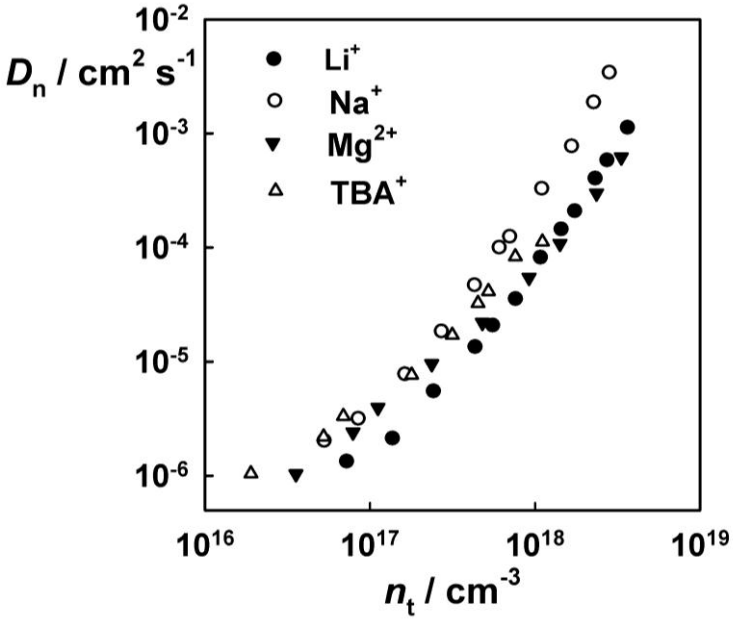

Figure 6. Effective electron diffusion coefficients measured for DSCs with different cations as a function of concentration of trapped electrons. Note that the plots should coincide if the trap distribution is independent of the cations.

Although the use of the trapped electron concentration as a reference framework for order of magnitude comparisons of DSC properties appears justified in the present case, the approach is not universally applicable. Major changes in electrolyte composition, e.g. substitution of organic solvents

by ionic liquids could alter the electron trap distribution significantly.[21]

Comparison of τ_n values

Since it is clear that the electron trap concentration and distribution are not significantly affected by the nature of the cations, a meaningful comparison of electron lifetimes can be made at constant electron trap occupancy, i.e. constant n_t. Figure 7 contrasts the τ_n values as a function of n_t. It can be seen that the τ_n plots for Na^+ and Li^+ are almost coincident, By contrast the plots for Mg^{2+} and TBA^+ show that the back reaction is considerably faster in these electrolytes. This is consistent with the results in Figure 4. In principle, adsorbed cations could influence the rate of electron back reaction in a number of ways. The first is by shielding the electron - I_3^- repulsion. The second is by increasing the local I_3^- concentration at the surface by electrostatic effects through intercalation/adsorption on the surface of TiO_2 particles.[38] Free cations could also influence the electron back reaction rate by the formation of ion pairs with I_3^-. In all cases, one would expect the effects to be most marked for cations with a high charge/radius ratio. The trend in τ_n for the inorganic cations Na^+, Li^+ and Mg^{2+} is consistent with this interpretation, but the result for TBA^+ is surprising. Theoretical calculations by Kusama *et al.* indicate that large cations such as TBA^+ in the electrolyte could slow down regeneration of the dye. According to these calculations, when compared to smaller cations such as Li^+, TBA^+ exhibits a weaker interaction between the oxidized dye (D^+) and iodide species (I^- or I_2^-) *via* the S atom in the SCN ligand of N719.[39] However, slow dye regeneration cannot explain the present results since the back reaction of electrons with D^+ is expected to be important only at high intensities, where it will be manifest as an apparent reduction in injection efficiency. This could reduce the open circuit voltage still further. These effects may also be influenced by interactions between cations and TBP, as suggested by Katoh *et al*.[40]

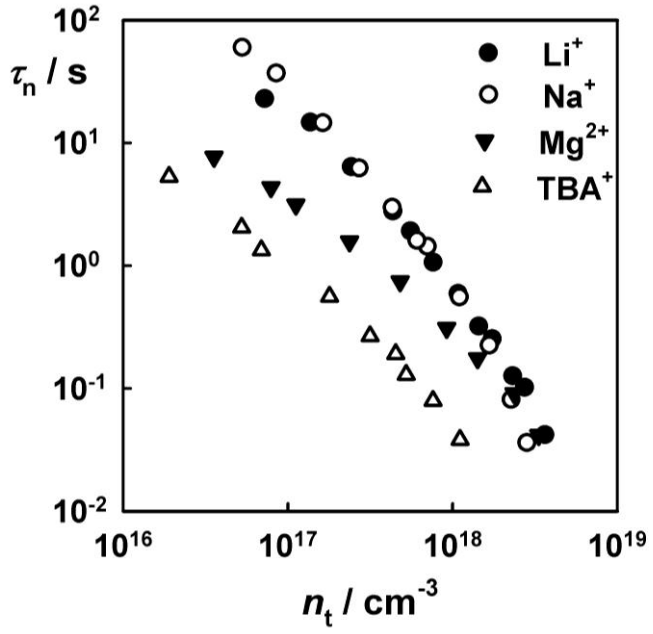

Figure 7. Variation of the apparent electron lifetime of DSCs with different cations as a function of concentration of trapped electrons.

Electron diffusion length

The methodology for determining the electron diffusion length by IMPS and IMVS has been described elsewhere.[21,41-43] It follows from equations 1 and 3 that the electron diffusion length $L_n = (D_n \tau_n)^{1/2}$ will be equal to $(D_{n,0} \tau_{n,0})^{1/2}$ since the $\partial n_t/\partial n_c$ terms cancel out. Figure 8 illustrates the L_n values for the different electrolytes as a function of voltage. It can be seen that the electrolyte containing Na^+ gives the largest electron diffusion length (above 100 μm) and TBA^+ the smallest (about 20 μm). At first sight the difference between the L_n values for Na^+ and Li^+ is surprising, but it is consistent with the observation that the D_n vs. n_t plot for Na^+ lies above the corresponding plot for Li^+ (cf. Fig 6). In both cases, the measured electron diffusion length is considerably larger than the film thickness, so that one would expect the short circuit collection efficiency to be close to 100%. The small differences in short circuit current (cf. Fig 1) and in the IPCE (cf. Figure 2) between Na^+ and Li^+ may therefore reflect subtle effects of the cation on the injection efficiency. Alternatively they could be a consequence of

differences in the reaction order for the recombination process.[32] By contrast, L_n in the TBA^+ electrolyte is so low that the collection efficiency will be considerably less, as is also evident from the short circuit current and IPCE. At the same time, we may expect that the injection efficiency in the TBA^+ electrolyte to also be less than 100% due to poor alignment of the TiO_2 conduction band with the LUMO of the dye.

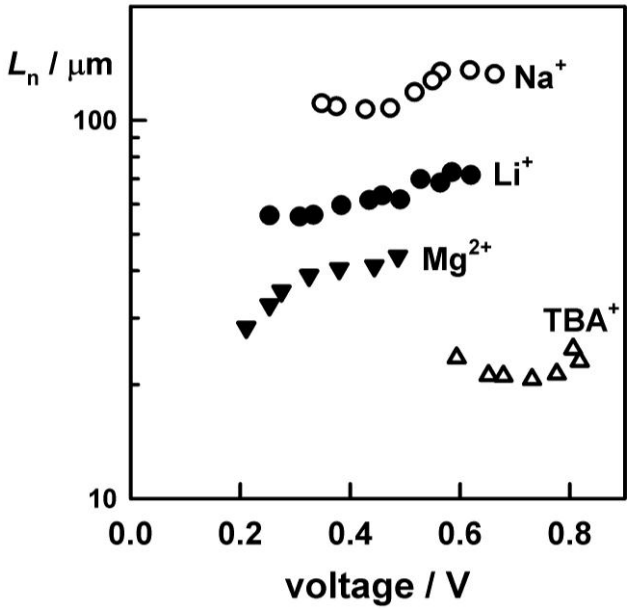

Figure 8. Electron diffusion lengths, L_n, of the DSC with electrolytes containing different cations.

An order of magnitude estimate of the $\tau_{n,0}$ values for the different electrolytes can be made by assuming that $D_{n,0}$ has the same value as in bulk anatase, 0.4 $cm^2\ s^{-1}$.[44] The $\tau_{n,0}$ values estimated in this way range from 0.4 ms for Na^+ to 10 μs for TBA^+. Estimates of the conduction band position based on extrapolation of plots of τ_n vs. voltage plots are subject to quite large errors due to the fact that the trap distribution is not exponential (cf. Fig 3), but approximate values are of $E_c - E_{F,redox}$ = 1.2 eV for the TBA^+ electrolyte and around 0.95 V for the Mg^{2+} electrolyte

Conclusions

The influence of electrolyte cations (Li^+, Na^+, Mg^{2+} and TBA^+) on DSC performance was investigated

by distinguishing their effect on the τ_n and D_n from their influence on the TiO_2 conduction band energy by employing the density of trapped electrons as a reference. This approach, which is based on the assumption that the electron trap distribution is the same in the four electrolytes studied, appears to be justified, since the D_n of the DSCs with different cations are similar (but not identical) when compared in this way. The best overall performance for cells using an acetonitrile/valeronitrile solvent mixture based electrolyte was obtained with the NaI electrolyte. Cells constructed using TBAI performed worst as a consequence of lower injection efficiency and short electron diffusion length. The methodology employed in this study should be useful for optimization of DSCs, but the assumption that the electron trap distribution is independent of changes in electrolyte composition needs to be tested in each case.

Acknowledgements

The authors thank EPSRC (UK) for financial support for this work.

References

(1) Wang, H. X.; Liu, M. N.; Zhang, M.; Wang, P.; Miura, H.; Cheng, Y.; Bell, J. *Phys. Chem. Chem. Phys.,* **2011**, *13*, 17359-17366.

(2) O'Regan, B.; Gratzel, M. *Nature* **1991**, *353*, 737-740.

(3) Liu, Y.; Hagfeldt, A.; Xiao, X. R.; Lindquist, S. E. *Sol. Energy Mater. Sol. Cells* **1998**, *55*, 267-281.

(4) Redmond, G.; Fitzmaurice, D. *J. Phys. Chem.* **1993**, *97*, 1426-1430.

(5) Enright, B.; Redmond, G.; Fitzmaurice, D. *J. Phys. Chem.* **1994**, *98*, 6195-6200.

(6) Kelly, C. A.; Farzad, F.; Thompson, D. W.; Stipkala, J. M.; Meyer, G. J. *Langmuir* **1999**, *15*, 7047-7054.

(7) Watson, D. F.; Meyer, G. J. *Coord. Chem. Rev.* **2004**, *248*, 1391-1406.

(8) Pelet, S.; Moser, J. E.; Gratzel, M. *J. Phys. Chem. B* **2000**, *104*, 1791-1795.

(9) Olson, C. L. *J. Phys. Chem. B* **2006**, *110*, 9619-9626.

(10) Haque, S. A.; Palomares, E.; Cho, B. M.; Green, A. N. M.; Hirata, N.; Klug, D. R.; Durrant, J. R. *J. Am. Chem. Soc.* **2005**, *127*, 3456-3462.

(11) Kambe, S.; Nakade, S.; Kitamura, T.; Wada, Y.; Yanagida, S. *J. Phys. Chem. B* **2002**, *106*, 2967-2972.

(12) Nakade, S.; Kanzaki, T.; Kambe, S.; Wada, Y. J.; Yanagida, S. *Langmuir* **2005**, *21*, 11414-11417.

(13) Wang, H. X.; Bell, J.; Desilvestro, J.; Bertoz, M.; Evans, G. *J. Phys. Chem. C* **2007**, *111*, 15125-

15131.

(14) Nakade, S.; Kanzaki, T.; Kubo, W.; Kitamura, T.; Wada, Y.; Yanagida, S. *J. Phys. Chem. B* **2005**, *109*, 3480-3487.

(15) Nakade, S.; Kanzaki, T.; Wada, Y.; Yanagida, S. *Langmuir* **2005**, *21*, 10803-10807.

(16) Kanzaki, T.; Nakade, S.; Wada, Y.; Yanagida, S. *Photochem. Photobiol. Sci.* **2006**, *5*, 389-394.

(17) Bisquert, J.; Vikhrenko, V. S. *J. Phys. Chem. B* **2004**, *108*, 2313-2322.

(18) Li, R. Z.; Liu, J. Y.; Cai, N.; Zhang, M.; Wang, P. *J. Phys. Chem. B* **2010**, *114*, 4461-4464.

(19) Shi, Y. S.; Wang, Y. H.; Zhang, M.; Dong, X. D. *Phys. Chem. Chem. Phys.* **2011**, *13*, 14590-14597.

(20) Nguyen, T. T. O.; Peter, L. M.; Wang, H. X. *Journal of Physical Chemistry C* **2009**, *113*, 8532-8536.

(21) Wang, H.; Peter, L. M. *J. Phys. Chem. C* **2009**, 113, 18125-18131.

(22) Bisquert, J.; Fabregat-Santiago, F.; Mora-Seró, I.; Garcia-Belmonte, G.; Giménez, S. *J. Phys. Chem. C* **2009**, *113*, 17278-17290.

(23) Cameron, P. J.; Peter, L. M. *J. Phys. Chem. B* **2003**, *107*, 14394-14400.

(24) Dloczik, L.; Ileperuma, O.; Lauermann, I.; Peter, L. M.; Ponomarev, E. A.; Redmond, G.; Shaw, N. J.; Uhlendorf, I. *J. Phys. Chem. B* **1997**, *101*, 10281-10289.

(25) Fisher, A. C.; Peter, L. M.; Ponomarev, E. A.; Walker, A. B.; Wijayantha, K. G. U. *J. Phys. Chem. B* **2000**, *104*, 949-958.

(26) Franco, G.; Gehring, J.; Peter, L. M.; Ponomarev, E. A.; Uhlendorf, I. *J. Phys. Chem. B* **1999**,

103, 692-698.

(27) Kato, Y.; Tada, K.; Onoda, M. *Jpn. J. Appl. Phys. 1* **2003**, *42*, 1458-1461.

(28) Zhang, S. F.; Yang, X. D.; Zhang, K.; Chen, H.; Yanagida, M.; Han, L. Y. *Phys. Chem. Chem. Phys.* **2011**, *13*, 19310-19313.

(29) Jennings, J. R. Ph.D. thesis, University of Bath 2009.

(30) Koops, S. E.; O'Regan, B. C.; Barnes, P. R. F.; Durrant, J. R. *J. Am. Chem. Soc.* **2009**, *131*, 4808-4818.

(31) Fredin, K.; Nissfolk, J.; Boschloo, G.; Hagfeldt, A. *J. Electroanal. Chem.* **2007**, *609*, 55-60.

(32) Villanueva-Cab, J.; Wang, H. X.; Oskam, G.; Peter, L.M. *J. Phys. Chem. Lett.* **2010**, *1*, 748-751.

(33) Lobato, K.; Peter, L. M.; Wurfel, U. *J. Phys. Chem. B* **2006**, *110*, 16201-16204.

(34) Lobato, K.; Peter, L. M. *J. Phys. Chem. B* **2006**, *110*, 21920-21923.

(35) Jennings, J. R.; Peter, L. M. *J. Phys. Chem. C* **2007**, *111*, 16100-16104.

(36) Boschloo, G.; Hagfeldt, A. *J. Phys. Chem. B* **2005**, *109*, 12093-12098.

(37) Kopidakis, N.; Schiff, E.A.; Park, N.G.; van de Lagemaat, J.; Frank, A.J., *J. Phys. Chem. B.* **2000**, *104*, 3930-3936.

(38) Boschloo, G.; Fitzmaurice, D. *J. Phys. Chem. B* **1999**, *103*, 7860-7868.

(39) Kusama, H.; Sugihara, H.; Sayama, K. *J. Phys. Chem. C* **2011**, *115*, 2544-2552.

(40) Katoh, R.; Kasuya, M.; Kodate, S.; Furube, A.; Fuke, N.; Koide, N., *J. Phys. Chem. C* **2009** *113*, 20738-20744.

(41) Jennings, J. R.; Ghicov, A.; Peter, L. M.; Schmuki, P.; Walker, A. B. *J. Am. Chem. Soc.* **2008**,

130, 13364-13372.

(42) Peter, L. M. *J. Phys. Chem. C* **2007**, *111*, 6601-6612.

(43) Dunn, H. K.; Peter, L. M. *J. Phys. Chem. C* **2009**, *113*, 4726-4731.

(44) Forro, L.; Chauvet, O.; Emin, D.; Zuppiroli, L.; Berger, H.; Lévy, F. *J. Appl. Phys.* **1994**, *75*, 633-635.

Table of Content